Infectious Disease Modelling 6 (2021) 532–544

Contents lists available at ScienceDirect

Infectious Disease Modelling

journal homepage: www.keaipublishing.com/idm

Bertalanffy-Pütter models for the first wave of the COVID-19 outbreak

Norbert Brunner, Manfred Kühleitner*

University of Natural Resources and Life Sciences (BOKU), Department of Integrative Biology and Biodiversity Research (DIBB), A-1180, Vienna, Austria

ARTICLE INFO

Article history:
Received 28 October 2020
Received in revised form 8 March 2021
Accepted 8 March 2021
Available online 13 March 2021
Handling editor: Dr. J Wu

Keywords:
Akaike information criterion (AIC)
Bertalanffy-Pütter model (BP-Model)
COVID-19 pandemic
Epidemic trajectory
Least-squares method
Simulated annealing algorithm

ABSTRACT

The COVID-19 pandemics challenges governments across the world. To develop adequate responses, they need accurate models for the spread of the disease. Using least squares, we fitted Bertalanffy-Pütter (BP) trend curves to data about the first wave of the COVID-19 pandemic of 2020 from 49 countries and provinces where the peak of the first wave had been passed. BP-models achieved excellent fits (R-squared above 99%) to all data. Using them to smoothen the data, in the median one could forecast that the final count (asymptotic limit) of infections and fatalities would be 2.48 times (95% confidence limits 2.42–2.6) and 2.67 times (2.39–2.765) the total count at the respective peak (inflection point). By comparison, using logistic growth would evaluate this ratio as 2.00 for all data. The case fatality rate, defined as the quotient of the asymptotic limits of fatalities and confirmed infections, was in the median 4.85% (confidence limits 4.4%–6.5%). Our result supports the strategies of governments that kept the epidemic peak low, as then in the median fewer infections and fewer fatalities could be expected.

1. Introduction

Modeling approaches

The first wave of the novel COVID-19 disease has challenged governments across the world. Most states reacted swiftly, closing borders, and imposing stay-at-home rules. Within a few weeks they could curb the further spread of the coronavirus SARS-CoV2, but the economic costs were high. In the meantime, new waves emerged, and we ask: What lessons could be drawn from the first wave?

This paper focuses on epidemic modeling using trend analysis, but with a goal that differs from the common applications of this method. Rather than using trend-lines for the forecasting of epidemic trajectories we used them to smoothen the data, because the data might have been blurred by random fluctuations and errors (e.g. delays in reporting). The smooth curves were then used to derive certain statistics for the time-series of infections.

* Corresponding author. Institute of Mathematics, DIBB, BOKU Gregor Mendel Strasse 33, A-1180, Vienna, Austria.
E-mail address: manfred.kuehleitner@boku.ac.at (M. Kühleitner).
Peer review under responsibility of KeAi Communications Co., Ltd.

https://doi.org/10.1016/j.idm.2021.03.003

Trend analysis was already applied successfully for the modeling of COVID-19. For example, exponential (Malthusian) growth has been used to describe the initial explosive spread of infections (Remuzzi & Remuzzi, 2020). However, exponential growth is not suitable for the modeling of data with a peak. Such data need models with sigmoidal (S-shaped) growth curves. For this purpose, the Verhulst (1838) model of logistic growth has been particularly popular (Google scholar: about 250 papers per month about "COVID-19" and "logistic growth"). Logistic growth has achieved good fits to data from China (Shen, 2020) and Italy (Vattay, 2020), but for other data the fit has not been that good (Kamrujjaman et al., 2020).

A major drawback of the logistic model is the inflexibility with respect to the inflection point: At the peak of the outbreak (inflection point) the logistic model predicts a doubling of the current cumulated count as the final size of the disease (asymptotic size). Thus, logistic growth was not suitable for the study of the ratio of asymptotic size over peak size, because for logistic growth this ratio is fixed independently of the actual data and the actual policy responses. (A similar argument applies to many more growth models, e.g. Brody or Gompertz.) Realistic forecasts for this ratio can only be expected from models that are more flexible with respect to the relation between the inflection point (peak) and the asymptotic limit (final size).

We therefore use the Bertalanffy-Pütter (BP) model to describe the growth of COVID-19. Its growth curves are solutions of differential equation (1). The model was introduced by Pütter (1920). Bertalanffy (1957) popularized it for modeling animal growth and Chowell (2017) introduced it into epidemiology under the name "generalized Richards model". It was recently used to describe the first wave of COVID-19 in China (Wu et al., 2020).

$$y'(t) = p \cdot y(t)^a - q \cdot y(t)^b \tag{1}$$

Equation (1) describes cumulative case-counts by a function $y(t)$ of time (t in days). Thereby, $t = 0$ represents the first datapoint and the five free model parameters are the non-negative exponent-pair $a < b$ (logistic growth: $a = 1$, $b = 2$), non-negative scaling constants p and q, and the initial value $y(0) = c > 0$. ("Free" means that the parameters are determined from fitting the model to the data.)

Problem of the paper

First, we explored the goodness of fit of the five-parameter BP-model (1) to COVID-19 data. We selected a sample of 49 countries and provinces, whose data for the first wave displayed a peak, i.e. during the first wave the countries had succeeded in "flattening the curve". Using the method of least squares, for each country/province we fitted BP-models to two time-series, cumulated counts of fatalities and of confirmed cases (diagnosed infections).

Second, for each country and time-series (confirmed cases, fatalities) we used the BP-models to compute certain statistics of practical significance and study them with statistical methods, such as the asymptotic limits (final sizes of the first wave), the inflection points (peaks of the first wave) and statistics computed from them, specifically final size over peak size. Given the sample of 49 countries/provinces, which value of this ratio was typical for the first wave of COVID-19? Could we distinguish between countries that had a good or a poor performance during the first wave of COVID-19?

Third, to explore the utility of BP-models for forecasting, we fitted it to the initial half of the data and compared its extrapolation with the actual epidemic trajectories. For this purpose, we considered a calibration by means of weighted least squares using a new weighing scheme.

2. Method

Data

We retrieved the data for this paper from CSSE (2020). This source collects for various entities (countries and provinces) the daily counts of confirmed infections, of deaths and of recovered patients, and it updates this information daily. However, for several countries the source does not record the count of recovered patients, whence for this paper for each of 49 countries and provinces we used two time-series, fatalities and confirmed cases. To ensure reproducibility of our data, we defined a reference day (June 18, 2020), so that each time-series started at the first nonzero entry for that country/province (indicator cases and first fatalities, respectively) and it terminated on the reference day (Table 1). The resulting time-series reported daily counts for 47–148 days.

The time-series for the confirmed infections in the Chinese province of Hubei was insofar exceptional, as it started with 444 confirmed cases. (As the pandemic started in Hubei and the disease was unknown then, the earlier counts were obtained with different methods and the source had removed the initial segment of this time-series; the same for the fatalities.) Further, the data for the USA pertain mainly to the first wave in the Northeast, where a "flattening of the curve" was discernable, although the first wave in the other states just has begun.

For the choice of our sample of countries, we selected only countries/provinces that had succeeded in the flattening of the growth curve prior to the reference day. (Thus, the epidemic peak and the final size could be discerned roughly.) We used this criterion because our research question relates the peak to the final size. Further, we wished to utilize the observation that BP-type models would be particularly suitable for the modeling of data that include the after-peak stage (Sornette et al., 2020).

Table 1
Summary of the data.

Country	Fatalities			Confirmed cases		
	Start	n_D = days	June 18	Start	n_C = days	June 18
Andorra	March 22	88	52	March 2	108	854
Australia: New South Wales	March 4	106	48	January 26	144	3137
Austria	March 12	98	687	February 25	114	17,203
Belgium	March 11	99	9675	February 4	135	60,244
Burkina Faso	March 18	92	53	March 10	100	899
Canada: Alberta	March 20	90	151	March 6	104	7530
Canada: British Columbia	March 9	101	168	January 28	142	2775
Canada: Nova Scotia	April 7	72	62	March 16	94	1061
Canada: Ontario	March 17	93	2607	January 26	144	34,382
Canada: Quebec	March 19	91	5298	February 28	111	54,263
Chad	April 28	51	74	March 19	91	854
China: Hubei	January 22	86	3222	January 22	148	68,135
Croatia	March 19	91	107	February 25	114	2258
Cuba	March 18	92	84	March 12	98	2280
Czechia	March 22	88	333	March 1	109	10,162
Denmark (mainland)	March 14	96	598	February 27	112	12,294
Estonia	March 25	85	69	February 27	112	1977
Finland	March 21	89	326	January 29	141	7117
France (mainland)	February 15	124	29,512	January 24	146	189,906
Germany	March 9	101	8851	January 27	143	188,604
Greece	March 11	99	187	February 26	113	3203
Hungary	March 15	95	567	March 4	106	4078
Ireland	March 11	99	1710	February 29	110	25,341
Israel	March 21	89	303	February 21	118	19,783
Italy	February 21	118	34,448	January 31	139	237,828
Japan	February 13	126	935	January 22	148	17,530
Luxembourg	March 14	96	110	February 29	110	4085
Malaysia	March 17	93	121	January 25	145	8515
Morocco	March 10	100	213	March 2	108	8997
Netherlands (mainland)	March 6	104	6074	February 27	112	49,204
Niger	March 25	85	67	March 20	90	1020
Norway	March 14	96	243	February 26	113	8692
Portugal	March 17	93	1523	March 2	108	37,672
San Marino	March 3	107	42	February 27	112	696
Sierra Leone	April 23	56	51	March 31	79	1249
Slovenia	March 14	96	109	March 5	105	1503
South Korea	February 20	119	280	January 22	148	12,257
Spain	March 3	107	28,752	February 1	138	244,683
Sweden	March 11	99	5041	January 31	139	54,562
Switzerland	March 5	105	1956	February 25	114	31,187
Tajikistan	May 2	47	51	April 30	49	5221
Thailand	March 1	109	58	January 22	148	3135
Tunisia	March 19	91	50	March 4	106	1128
UK (mainland)	March 6	104	42,153	January 31	139	299,251
UK: Channel Island	March 26	84	48	March 10	100	570
UK: Isle of Man	April 1	78	24	March 20	90	336
United Arab Emirates	March 20	90	295	January 29	141	43,364
Uruguay	March 28	82	24	March 13	97	849
USA (mainland)	February 29	110	117,717	January 22	148	2,163,290

Source: CSSE (2020).

Moreover, we aimed at a sample that represents all parts of the world, including extremely poor and rich countries (e.g. Burkina Faso and Norway). Also the demographic structure of the countries differed (the case fatality rate is known to increase with age), as did their medical infrastructures (e.g. access to intense care units), and the transmission patterns (e.g., ethnic and socio-economic factors, social interactions and clusters may matter). Consequently, for the countries of our sample the reactions to and experiences with COVID-19 varied widely, from a lockdown in the Chinese province of Hubei to mere appeals for more personal responsibility in Sweden, from intense care units that remained below their capacity in Austria to a breakdown of the public health system in Italy.

As official COVID-19 data may be distorted for political reasons, we used an independent and well-esteemed source (CSSE, 2020). However, there remained a problem of underreporting, as a peculiarity of COVID-19 is the large number of asymptotic carriers. According to one source (Ferretti et al., 2020), up to 50% of COVID-19 infections may happen from carriers that have not developed symptoms yet. Further, the pre-symptomatic incubation period is relatively long (WHO, 2020.) Thus, to detect and insulate infected persons depends largely on the intensity of testing, which in turn may vary considerably over time (e.g. initial shortage of test kits) and between countries. (Thus, in China 86% of infections may have remained undetected prior to

the lockdown of Wuhan: Li et al., 2020.) To reduce this type of inevitable data uncertainty, we used two time-series per country in parallel, death tolls in addition to the counts of confirmed infections, as we did not expect a significant number of undetected COVID-19 deaths. However, the two trajectories did not develop perfectly in parallel, as the case fatality rate increased significantly, when in some countries the public health systems were overcharged (Vattay, 2020).

Calibration and model selection

We used the (ordinary) least-squares method, which is the most common tool of calibration, and variants of it. It measures the goodness of the fit to the data by means of *SSE*, the sum of squared errors (fit residuals) in equation (2). We sought five parameters (a, b, c, p, q), so that for the solution $y(t)$ of equation (1) the following sum *SSE* was minimized, whereby y_i was the total count up to time t_i and n was the length of the time-series of data-points:

$$SSE = \sum_{i=1}^{n} (y_i - y(t_i))^2 \tag{2}$$

In the context of forecasting we developed an alternative measure for the goodness of fit, weighted least-squares that aimed at finding parameters to minimize the following sum (3) of weighted squared errors *SWSE*:

$$SWSE = \sum_{i=1}^{n} \frac{(y_i - y(t_i))^2}{|y(\acute{t}_i)|} \tag{3}$$

Another measure for the goodness of fit related to *SSE* is the coefficient of determination, R-squared (R^2) of equation (4). It compares the model-fit with the fit by the trivial constant model (relative improvement) and can be used to assess the goodness of fit across different datasets.

$$R^2 = 1 - \frac{SSE}{\sum_{k=1}^{n} (y_k - mean(y_1, y_2, \ldots y_n))^2} \tag{4}$$

In view of certain limitations for the interpretation of R-squared, in this paper we did not use it for model-selection. For such a purpose the Akaike information criterion (*AIC*), equation (5), was shown to be more selective (Spiess & Neumeyer, 2010). We therefore used *AIC* for model comparison and used R-squared merely to inform about the goodness of fit by means of a well-known statistic.

$$AIC = n \cdot \ln\left(\frac{SSE}{n}\right) + 2 \cdot K \tag{5}$$

Here, n is the number of data-points and K is the number of optimized parameters of the model. ($K = 6$ for the general BP-model, counting a, b, c, p, q and *SSE*, and $K = 4$ for logistic growth, where $a = 1, b = 2$ are not optimized.) When comparing two models, the model with the lower *AIC* is selected (Burnham & Anderson, 2002; Motulsky & Christopoulos, 2003), whereby *AIC* penalizes the model with more parameters. When comparing a model with the best-fit model (*AIC* and AIC_{min}, respectively), then equation (6) computes the probability, $\wp$, that the (worse) model with higher *AIC* would be "true", when compared to the model with the least *AIC* (Burnham & Anderson, 2004). Note that a difference of *AIC* above 10 strongly supports the refutation of the model with a higher *AIC* ($\wp < 0.7\%$).

$$\wp = \frac{\exp\left(-\frac{AIC - AIC_{min}}{2}\right)}{1 + \exp\left(-\frac{AIC - AIC_{min}}{2}\right)} \tag{6}$$

BP-model and optimization

The BP-model generalizes several well-known models. Special cases are the Brody (1945) model of bounded exponential growth with exponent-pair $(a, b) = (0, 1)$, Verhulst (1838) logistic growth with pair (1, 2), or the model of von Bertalanffy (1957) with (2/3, 1). The Gompertz (1832) model fits into this scheme, too: It is the limit case of the pair (1, 1), but with a different differential equation (Marusic & Bajzer, 1993). Equation (1) also includes several models with four free parameters, such as the generalized Bertalanffy model ($b = 1$ with $0 \leq a < 1$ variable), the Richards (1959) model ($a = 1$ with $b > 1$ variable), or the generalized logistic model ($b = a+1$ with $a > 0$ variable; c.f. Roosa et al., 2020).

For the BP-model, the relation between the asymptotic limit (size) y_{max} and the inflection point at time t_{infl} with size y_{infl} is given by equations (7) and (8). Thereby, the asymptotic limit estimates the final size of (the first wave of) the disease; the inflection point represents the peak of (the first wave of) the epidemics. If $q = 0$, then the growth function is unbounded, and if $a = 0$, then there is no inflection point.

$$y_{max} = \left(\frac{p}{q}\right)^{\frac{1}{b-a}} \quad \text{if } q > 0 \tag{7}$$

$$y_{infl} = \left(\frac{a}{b}\right)^{\frac{1}{b-a}} \cdot y_{max} \quad \text{if } a > 0 \text{ and } q > 0 \tag{8}$$

As follows from equation (8), for logistic growth the ratio y_{max}/y_{infl} is fixed (ratio = 2, because $a = 1$, $b = 2$), whereas for model (1) with variable exponent-pairs any ratio larger than 1 can be attained. Further, model (1) always fits better to the data than the logistic growth model, as it generalizes this model. (The same for any other three-parameter BP-model with given exponent-pair.)

For certain BP-models with three or four parameters, there are different parametrizations that aim at describing model (1) in terms of growth parameters that are meaningful for animals (c.f. Tjørve & Tjørve, 2017). For the general five-exponent BP-model, such parametrizations are not available, as although equation (1) can be solved analytically, non-elementary functions are needed for the solution of the general equation (Ohnishi et al., 2014).

Standard optimization tools did not always identify the best-fit parameters for the five-parameter BP-model. We therefore used a custom-made optimization method using the Mathematica code from Renner-Martin et al. (2018). The method searches the best-fit exponent-pair on a given search-grid (which is adapted during optimization) and for each fixed grid-point exponent-pair (a, b) it uses a variant of simulated annealing to identify the best-fitting remaining parameters (c, p, q). Simulated annealing (Vidal, 1993) uses elements of a random search to escape a suboptimal local minimum, which is an advantage in the presence of many local optima (as for the present optimization problem). This approach identified BP-model parameters with growth curves close to the data.

Statistical analysis

For each dataset, we used the best-fit BP-model to compute various statistics. For example, the ratios y_{max}/y_{infl} for the time series of fatalities defined a random sample (of size 49) and we then used standard methods from statistics to further analyze this sample. Note that our paper aimed at a comparison of countries in terms of these COVID-19 statistics, following the example of literature in comparative international law (e.g. Brunner & Tschohl, 2014; Hathaway, 2002; Magesan, 2013). Therefore, we were not interested in the variability of a statistic for a single time-series, but we studied the variability of a statistic across different the time-series for different countries.

In view of the unknown distributions and the small sample size, we used primarily non-parametric methods, e.g. Spearman rank test for correlations, Siegel-Tukey-test for the variance, sign-test for location parameters. (The true distributions of our statistics were most likely complicated; c.f. ratio-distributions in Díaz-Francés & Rubio, 2013.)

In this paper, all confidence intervals assume 95% confidence. When we used nonparametric tests to establish confidence intervals, we also informed about the actual (higher) level of confidence. For instance, when we used the one-sided sign test for the confidence interval of a median (Hollander, 1999), we informed about the P-values of the lower and upper confidence limits, as in view of the discrete nature of the test these were not always equal.

For some statistics we were interested in their distributions. Thereby, we used the Anderson-Darling-test to check certain simple assumptions for continuous distributions. (For distributions different from the normal distribution we applied this test using 5000 Monte-Carlo simulations.) For a P-value below 5% we refuted the distribution assumption. To check, if the underlying distribution of samples A and B differed, we tested, if sample A was distributed according to the smooth kernel distribution of sample B.

3. Results and discussion

R-squared of the best-fit BP-model curves

Table 2 and Table 3 lists the best-fit parameters of the BP-model and inform about the goodness of fit: Note that other than suggested by Chowell (2017), optimization needed exponents $a > 1$. For the 49 time-series of fatalities, R-squared ranged between 99.06% and 99.98% and for the time-series of confirmed cases R-squared ranged between 98.46% and 99.97%. R-squared could be interpreted as a statistic associated to each time-series. Under this viewpoint, the median of the pooled R-squared values (i.e. 98 values) was 99.83%. The lower and upper confidence limits for the median were 99.785% and 99.865%. (For each of these limits a one-sided sign-test for the hypothesis that this limit would be a median resulted in the P-value 1.668%, whence the actual confidence level was 96.7%.)

For logistic growth, the fit was excellent, too, with the 98 R-squared values in the range between 96.50% and 99.93%. While the R-squared values for logistic growth were smaller, but still comparable to those of the best-fit BP-model, the Akaike

Table 2
Best-fit BP-parameters, goodness of fit, and comparison with logistic growth for the cumulative counts of deceased.

Country	Parameters					Goodness of fit		Logistic	
	a	b	c	p	q	SSE	R^2	ΔAIC	R^2
Andorra	0.52	0.96	1.02E-01	9.15E-01	1.60E-01	7.59E+01	99.66%	130.3	98.45%
AU: NSW	0.52	4.92	3.24E-01	2.00E-01	7.96E-09	2.42E+02	99.30%	4.9	99.24%
Austria	0.82	1.20	6.74E-02	6.83E-01	5.76E-02	7.30E+03	99.88%	135.0	99.50%
Belgium	0.99	1.14	1.14E+00	6.31E-01	1.60E-01	1.04E+06	99.93%	168.7	99.58%
Burkina Faso	0.21	2.94	8.83E-02	7.15E-01	1.36E-05	7.42E+01	99.73%	70.6	99.39%
CAN: Alberta	0.45	2.36	8.62E-04	5.78E-01	3.81E-05	5.77E+02	99.78%	77.9	99.45%
CAN: BC	0.90	1.05	5.23E-01	5.00E-01	2.29E-01	7.75E+02	99.79%	103.2	99.40%
CAN: NS	0.93	1.29	3.66E-01	3.91E-01	8.85E-02	7.91E+01	99.78%	43.1	99.58%
CAN: ONT	0.85	1.20	8.15E-02	5.38E-01	3.38E-02	4.78E+04	99.95%	167.7	99.65%
CAN: QU	0.80	1.19	6.70E-02	6.68E-01	2.24E-02	2.22E+05	99.93%	176.2	99.52%
Chad	0.63	1.01	6.78E-01	1.27E+00	2.49E-01	1.53E+02	99.43%	41.3	98.61%
China: Hubei	0.99	1.34	2.27E+01	3.52E-01	2.09E-02	7.22E+04	99.94%	90.8	99.81%
Croatia	0.72	2.18	7.13E-01	2.39E-01	2.64E-04	2.78E+02	99.80%	26.8	99.72%
Cuba	1.02	1.81	7.70E-01	1.40E-01	4.24E-03	6.80E+01	99.93%	9.1	99.92%
Czechia	0.59	0.99	1.54E-01	1.39E+00	1.35E-01	1.96E+03	99.81%	174.4	98.59%
Denmark	0.75	1.07	1.41E-01	9.00E-01	1.16E-01	2.86E+03	99.93%	218.4	99.32%
Estonia	0.43	1.08	5.35E-02	9.06E-01	5.66E-02	1.10E+02	99.73%	143.4	98.49%
Finland	1.11	1.34	2.17E+00	2.21E-01	5.83E-02	3.60E+03	99.74%	21.0	99.65%
France	1.08	1.22	3.89E-01	2.88E-01	6.84E-02	2.36E+07	99.88%	129.7	99.63%
Germany	0.90	1.17	4.78E-01	6.51E-01	5.60E-02	4.90E+05	99.96%	215.2	99.63%
Greece	0.60	1.02	7.29E-02	8.27E-01	9.12E-02	9.59E+02	99.75%	169.7	98.53%
Hungary	0.79	1.26	1.89E-02	4.62E-01	2.31E-02	3.11E+03	99.93%	178.5	99.49%
Ireland	1.19	1.20	1.54E+00	2.41E+00	2.23E+00	7.99E+04	99.83%	29.0	99.76%
Israel	0.78	1.01	2.67E-01	9.59E-01	2.58E-01	1.55E+03	99.84%	153.8	99.04%
Italy	0.93	1.03	5.53E-01	1.13E+00	3.97E-01	1.04E+07	99.95%	281.7	99.42%
Japan	1.22	1.50	1.74E+00	6.23E-02	9.09E-03	1.47E+04	99.91%	7.4	99.90%
Luxembourg	0.77	1.14	2.63E-01	5.34E-01	9.32E-02	3.70E+02	99.74%	104.0	99.20%
Malaysia	0.43	1.08	2.57E-01	1.37E+00	6.12E-02	1.85E+02	99.85%	206.5	98.51%
Marocco	0.87	1.13	6.71E-02	5.62E-01	1.40E-01	2.52E+03	99.58%	102.2	98.79%
Netherlands	0.84	1.20	1.40E-01	7.61E-01	3.30E-02	1.49E+05	99.97%	277.3	99.61%
Niger	0.33	10.22	8.11E-01	3.88E-01	4.15E-19	8.20E+01	99.82%	64.1	99.60%
Norway	0.95	1.17	3.77E-01	5.46E-01	1.64E-01	9.25E+02	99.87%	103.1	99.62%
Portugal	0.63	0.96	8.82E-02	1.74E+00	1.51E-01	3.33E+04	99.86%	199.5	98.79%
San Marino	0.68	1.26	2.51E-02	4.84E-01	5.54E-02	1.15E+02	99.44%	69.9	98.89%
Sierra Leone	0.69	2.18	1.50E+00	2.78E-01	7.82E-04	5.62E+01	99.67%	18.1	99.51%
Slovenia	0.83	1.24	3.55E-02	4.45E-01	6.49E-02	1.74E+02	99.89%	134.7	99.53%
South Korea	0.71	1.75	4.43E+00	3.15E-01	9.19E-04	1.45E+03	99.86%	90.5	99.70%
Spain	0.90	1.12	4.00E-01	9.93E-01	1.05E-01	2.38E+07	99.81%	117.1	99.40%
Sweden	0.84	1.05	3.28E-01	7.63E-01	1.25E-01	3.55E+05	99.89%	177.4	99.29%
Switzerland	0.86	1.31	5.97E-02	5.66E-01	1.88E-02	1.14E+04	99.98%	265.6	99.75%
Tajikistan	0.31	3.32	9.68E-01	1.20E+00	1.00E-05	9.05E+01	99.20%	4.3	99.05%
Thailand	1.00	1.41	5.48E-03	3.14E-01	5.99E-02	1.01E+02	99.83%	103.0	99.56%
Tunesia	0.61	1.02	1.12E-01	7.56E-01	1.54E-01	1.64E+02	99.23%	76.1	98.15%
UK	0.95	1.02	8.53E-01	1.31E+00	6.22E-01	3.20E+07	99.88%	180.1	99.27%
UK: CI	1.26	1.41	1.04E+00	3.31E-01	1.87E-01	1.86E+02	99.20%	20.1	98.93%
UK: IM	1.46	1.59	2.65E-01	5.61E-01	3.72E-01	3.35E+01	99.49%	29.9	99.21%
UAE	1.19	1.36	1.26E+00	1.79E-01	6.82E-02	1.75E+03	99.84%	20.0	99.79%
Uruguay	0.00	3.16	8.68E-01	4.68E-01	1.97E-05	3.78E+01	99.06%	39.3	98.40%
USA	0.95	1.04	7.25E-01	9.12E-01	3.17E-01	1.50E+08	99.93%	220.5	99.44%

Notes: Countries the order of Table 1 (names abbreviated); x.xxE+/−yy means x.xx•$10^{+/-yy}$ (all numbers rounded to the two displayed decimals); $\Delta AIC = AIC$ (logistic model) minus AIC (best-fit BP-model).

information criterion indicated that logistic growth was false in comparison to the best-fit BP-model, except for one time-series (Canada, Alberta, cumulated confirmed cases). For 92 of the 98 time series, logistic growth was most likely false (AIC difference of 10 or higher).

The good fit of the general BP-model to all data confirmed the utility of our custom-made approach of grid-optimization, while well-established optimization tools failed to converge. An example for such a failure relates to the Levenberg-Marquart (LM) algorithm that was employed by Wu et al. (2020): In terms of R-squared, the supporting information of that paper reported for Shanghai $R^2 = 86.7\%$ for the five-parameter BP-model, while for logistic growth they reported the better fit $R^2 = 88.1\%$. Thus, the LM-algorithm failed to find the optimal model parameters for the five-parameter BP-model, because the general model necessarily should achieve a better fit than its special case of logistic growth.

Finally, we note that we fitted the model curve to the cumulated data and not to the daily new cases, which display much more random fluctuation and therefore results in a lower R-squared. By data-fitting to daily cases we mean the fitting of the temporal derivative $m'(t)$ to the daily data. In a different context we have shown that the growth curve $m(t)$ with the best fit to

Table 3
Best-fit BP-parameters, goodness of fit, and comparison with logistic growth for the cumulative counts of confirmed cases.

Country	Parameters					Goodness of fit		Logistic	
	a	b	c	p	q	SSE	R^2	ΔAIC	R^2
Andorra	0.89	1.34	2.77E-02	5.50E-01	2.77E-02	6.04E+03	99.94%	156.9	99.74%
AU: NSW	1.08	1.59	1.17E-02	2.00E-01	3.34E-03	2.55E+05	99.91%	33.1	99.89%
Austria	0.93	1.26	3.40E-01	6.55E-01	2.66E-02	2.17E+07	99.55%	68.3	99.15%
Belgium	1.09	1.18	6.34E-01	3.06E-01	1.14E-01	5.37E+07	99.94%	190.5	99.73%
Burkina Faso	0.63	0.91	1.63E-01	1.78E+00	2.63E-01	3.34E+04	99.63%	160.1	98.08%
CAN: Alberta	1.26	1.69	8.03E+01	2.59E-02	5.70E-04	2.52E+06	99.71%	−0.2	99.70%
CAN: BC	0.92	1.31	1.84E-02	2.57E-01	1.17E-02	6.60E+05	99.60%	100.2	99.17%
CAN: NS	0.64	3.08	7.63E+00	7.35E-01	3.08E-08	6.30E+03	99.96%	37.9	99.93%
CAN: ONT	0.97	1.27	1.81E-01	2.03E-01	8.61E-03	5.68E+07	99.74%	124.9	99.36%
CAN: QU	0.73	1.65	1.33E-02	1.10E+00	4.51E-05	3.59E+07	99.92%	134.2	99.73%
Chad	1.27	1.35	5.18E-01	2.41E-01	1.40E-01	1.53E+04	99.85%	6.8	99.84%
China: Hubei	0.61	4.09	9.87E+01	7.18E+00	1.10E-16	2.15E+08	99.63%	13.1	99.59%
Croatia	0.89	1.33	2.14E-02	4.93E-01	1.65E-02	5.62E+04	99.94%	186.0	99.68%
Cuba	0.9	1.08	8.07E-01	6.93E-01	1.73E-01	1.87E+05	99.71%	100.7	99.16%
Czechia	0.86	0.99	1.94E+00	1.46E+00	4.41E-01	9.92E+06	99.26%	99.0	98.09%
Denmark	0.89	1.04	1.81E+00	9.13E-01	2.22E-01	2.66E+06	99.88%	150.0	99.53%
Estonia	0.87	1.14	1.99E-01	6.77E-01	8.82E-02	2.03E+05	99.64%	88.6	99.19%
Finland	0.93	1.36	2.92E-02	2.40E-01	5.23E-03	3.93E+05	99.97%	248.3	99.79%
France	0.99	1.53	1.55E-01	2.18E-01	3.13E-04	2.21E+09	99.77%	43.8	99.68%
Germany	1.09	1.2	6.35E-01	2.59E-01	6.84E-02	1.56E+09	99.83%	134.7	99.54%
Greece	0.84	1.1	3.72E-01	8.38E-01	1.04E-01	4.93E+05	99.64%	116.0	98.97%
Hungary	0.92	1.14	5.17E-01	5.06E-01	8.08E-02	1.63E+05	99.94%	177.0	99.64%
Ireland	0.79	1.85	6.94E-03	7.85E-01	1.70E-05	9.19E+06	99.92%	51.0	99.87%
Israel	1.02	1.24	3.59E-01	3.69E-01	4.32E-02	1.04E+07	99.84%	99.8	99.60%
Italy	1.02	1.13	9.21E-01	4.45E-01	1.14E-01	7.31E+08	99.94%	258.6	99.63%
Japan	1.26	1.75	2.00E+01	2.07E-02	1.76E-04	9.37E+06	99.88%	32.2	99.85%
Luxembourg	0.93	1.21	2.19E-01	6.78E-01	6.66E-02	6.63E+05	99.74%	112.6	99.26%
Malaysia	0.93	1.29	1.41E-01	2.55E-01	9.89E-03	1.08E+07	99.29%	84.9	98.69%
Marocco	0.99	1.06	6.67E-01	7.45E-01	3.93E-01	1.03E+06	99.91%	136.7	99.67%
Netherlands	0.94	1.06	8.81E-01	9.91E-01	2.72E-01	3.25E+07	99.91%	178.7	99.56%
Niger	0.75	0.97	2.23E-01	1.66E+00	3.65E-01	1.60E+05	98.46%	70.0	96.50%
Norway	0.89	1.02	7.35E-01	1.42E+00	4.39E-01	1.48E+06	99.86%	178.2	99.32%
Portugal	0.89	0.9	1.26E+00	1.31E+01	1.18E+01	1.19E+08	99.33%	110.2	98.07%
San Marino	0.3	5.98	2.74E-04	1.99E+00	1.57E-16	1.72E+04	99.74%	63.5	99.53%
Sierra Leone	0.94	1.14	3.92E-01	3.62E-01	8.27E-02	2.57E+04	99.80%	48.8	99.62%
Slovenia	0.41	2.48	4.63E-05	3.62E+00	9.90E-07	1.74E+04	99.93%	152.0	99.70%
South Korea	0.99	1.27	2.65E-01	3.77E-01	2.77E-02	4.18E+07	98.66%	46.1	98.11%
Spain	1.06	1.22	4.78E-01	2.70E-01	3.72E-02	2.34E+09	99.84%	139.0	99.55%
Sweden	0.88	0.98	5.27E-01	5.91E-01	1.83E-01	1.55E+08	99.59%	118.4	99.01%
Switzerland	0.95	1.15	3.32E-01	8.17E-01	1.03E-01	6.67E+06	99.96%	240.6	99.66%
Tajikistan	1.01	1.3	6.69E+01	3.43E-01	2.84E-02	2.82E+05	99.82%	26.0	99.67%
Thailand	1.1	1.45	4.51E-02	1.66E-01	9.99E-03	4.07E+05	99.85%	82.7	99.74%
Tunesia	0.83	1.29	4.21E-02	6.27E-01	2.53E-02	3.86E+04	99.79%	116.7	99.33%
UK	1.01	1.2	6.92E-01	2.46E-01	2.23E-02	9.18E+08	99.95%	236.7	99.71%
UK: CI	0.88	1.3	2.12E-02	6.37E-01	4.47E-02	5.81E+03	99.87%	90.9	99.66%
UK: IM	1.05	1.35	4.51E+00	3.67E-01	6.42E-02	2.95E+03	99.74%	19.4	99.66%
UAE	0.91	1.43	7.87E-02	2.10E-01	7.00E-04	1.84E+07	99.94%	111.7	99.85%
Uruguay	0.21	0.57	1.64E+00	1.32E+01	1.10E+00	2.46E+04	99.58%	182.4	97.16%
USA	1.01	1.08	8.09E-01	4.51E-01	1.61E-01	1.77E+11	99.79%	165.4	99.33%

Note as for Table 2.

the cumulated data may be suitable to model the daily data, too, if a time-shift t_s is added (Ziegler et al., 2020). The reason, why some authors prefer fitting $m'(t)$ to daily data rather than fitting $m(t)$ to cumulated data is the possible underestimation of the size of the confidence intervals for the parameters (Shen, 2020). This problem does not matter for this paper, as we focus on comparisons of countries.

As for a limitation, note that the grid-optimization of this paper was not suitable to compute confidence intervals for the best-fit BP-model parameters to a particular time-series. The reason is the CPU-time needed for optimization: To estimate confidence intervals, the optimization would have to be repeated for several hundred random perturbations of the data. However, for the problem of this paper such confidence bounds were not needed, as we used the best-fit model merely to smoothen the data by means of a sigmoidal growth function and compute the inflection point. Thereby, we were not interested in the variability of the inflection point with respect to a specific time-series (confidence bounds), because we compared the inflection points from different time-series of different countries, where we expected a much higher variability.

Asymptotic limits and forecasting from subsamples

Fig. 1 illustrates a difficulty in estimating the final size of the first wave. The cumulated counts of fatalities in Austria (blue dots) continued to increase slowly, as the epidemics did not end with the first wave. (Specifically, there was a jump at $t = 76$ from 645 to 668 fatalities.) Therefore, there was no clear-cut definition of the "end of the first wave" and of its final size. We explored this issue by comparing for two calibrations (*SSE* and *SWSE*) the BP-model growth curves fitted to the full data (96 data-points) and the one fitted to the initial half of the data (48 data-points). For *SSE*, the growth curves fitted well to the first 55 data-points and to the data-points after the jump. Thereby the curve fitted to the initial 48 data-points (red solid line) had a slightly lower asymptotic limit than the one fitted to the full data (black solid line). This observation generalizes, as for *SSE* the asymptotic limit computed for an initial segment of the data in general underestimates the final size (Kühleitner et al., 2019). Thus, *SSE* could be used if all data-points came from the first wave. The growth curve for *SWSE* that was fitted to the initial 48 data-points (dashed red line) appeared to fit best to the initial 76 data-points, but it fitted poorly to the data-points after the above-mentioned jump. Thus, this growth curve could be used, if the first wave ended prior to the jump. The growth curve for *SWSE* that was fitted to the full data (dashed black line) appeared to fit worst, whereby the weights for *SWSE* by design tolerate a higher variability in the total count during the epidemic peak (where data uncertainty might be largest).

In view of the similar behavior of the two growth curves for *SSE* (solid lines) and the problematic fit of the latter *SWSE* growth curve, we decided to analyze the country performances by fitting a BP-growth curve to the full data and use *SSE* for calibration.

In the following sense this decision led us to implicitly assume that for our data the first wave lasted till the reference day (June 18) or ended only shortly before it. For, in the median over the considered time-series the cumulated counts on the reference day (Table 1), i.e. the maximal count $\max(y_i)$, differed barely from the asymptotic limits y_{max} of the BP-model curves that were fitted to the 98 time-series (Table 4). Thereby, equation (7) was used to compute y_{max} and we used the quotients $y_{max}/\max(y_i)$ as a test-statistic (Table 5). For the combined sample of 98 quotients, the median of the quotients was 0.994, whereby the lower and upper confidence limits were 0.9865 and 1. (The P-values of one-sided sign-tests were 1.668% and 2.72%, respectively, amounting to 95.6% confidence.) Thus, in the median the quotients were close to one, but slightly smaller. (This was to be expected, as the epidemics continued after the first wave.)

Notably, the different types of time-series differed with respect to the quotients $y_{max}/\max(y_i)$: The variance of the two samples of 49 quotients, one for fatalities and the other for confirmed cases, differed significantly (Siegel-Tukey test: P-value close to 0). Indeed, 95%of the quotients for the time-series of fatalities were in the interval between 0.954 and 1.131 (2.5% and 97.5% quantiles), while the same interval for the confirmed cases had the endpoints 0.871 and 2.013.

Forecasting the final size from the peak

We utilized the good approximation of the data by BP-growth functions (calibration: *SSE*) to obtain estimates for the peak y_{infl} (inflection point) from equation (8). Next, when comparing the final size and the peak size of the first wave of the epidemics we could ask: What forecast about the final size could be drawn at the peak, i.e.: how many further victims were to be

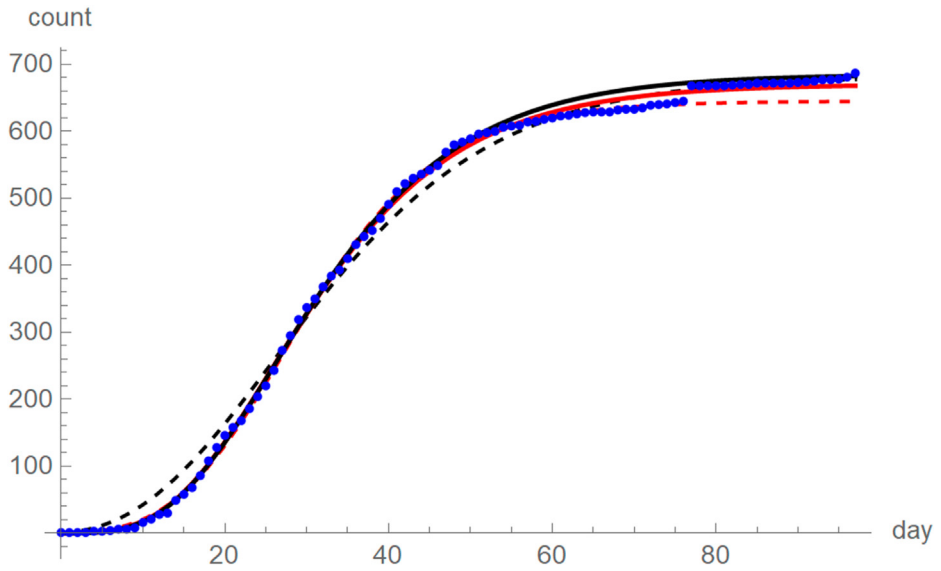

Fig. 1. Total count of deceased since the begin of the COVID-19 epidemics in Austria (blue dots), and four lines for the BP-model growth-curves with best fit to 100% (black) and 50% (red) of the data, using *SSE* (solid) and *SWSE* (dashed) for calibration.

Table 4
Further parameters (computed from the best-fit BP-model parameters).

Country	*fatalities*			*confirmed cases*		
	y_{max}	y_{infl}	t_{infl}	y_{max}	y_{infl}	t_{infl}
Andorra	5.25E+01	1.30E+01	10.64	7.63E+02	3.07E+02	26.90
AU: NSW	4.81E+01	2.89E+01	46.72	3.06E+03	1.43E+03	61.35
Austria	6.70E+02	2.46E+02	25.79	1.64E+04	6.52E+03	30.02
Belgium	9.60E+03	3.75E+03	32.79	5.94E+04	2.46E+04	64.83
Burkina Faso	5.36E+01	2.04E+01	19.20	9.33E+02	2.51E+02	20.61
CAN: Alberta	1.55E+02	6.49E+01	32.65	7.19E+03	3.63E+03	47.48
CAN: BC	1.83E+02	6.53E+01	36.12	2.74E+03	1.11E+03	68.19
CAN: NS	6.21E+01	2.50E+01	20.75	1.06E+03	5.54E+02	30.01
CAN: Ontario	2.73E+03	1.02E+03	40.65	3.74E+04	1.52E+04	92.65
CAN: Quebec	6.06E+03	2.19E+03	45.08	5.89E+04	2.43E+04	57.34
Chad	7.30E+01	2.11E+01	8.21	8.76E+02	4.08E+02	56.06
China: Hubei	3.21E+03	1.35E+03	22.10	6.79E+04	3.93E+04	20.33
Croatia	1.06E+02	4.96E+01	33.97	2.25E+03	9.02E+02	36.00
Cuba	8.34E+01	4.04E+01	34.28	2.25E+03	8.15E+02	33.83
Czechia	3.41E+02	9.36E+01	16.38	9.69E+03	3.28E+03	30.12
Denmark	6.05E+02	1.99E+02	24.17	1.25E+04	4.43E+03	38.38
Estonia	7.13E+01	1.73E+01	11.98	1.90E+03	6.97E+02	31.19
Finland	3.26E+02	1.44E+02	32.38	7.33E+03	3.03E+03	75.24
France	2.89E+04	1.21E+04	54.82	1.84E+05	8.22E+04	73.29
Germany	8.84E+03	3.35E+03	35.13	1.82E+05	7.60E+04	65.29
Greece	1.91E+02	5.39E+01	21.16	3.01E+03	1.07E+03	30.59
Hungary	5.84E+02	2.16E+02	37.93	4.17E+03	1.57E+03	41.86
Ireland	1.69E+03	7.31E+02	40.18	2.52E+04	1.13E+04	44.99
Israel	3.02E+02	9.80E+01	20.62	1.71E+04	7.03E+03	42.47
Italy	3.47E+04	1.25E+04	39.99	2.37E+05	9.33E+04	58.40
Japan	9.64E+02	4.61E+02	78.27	1.68E+04	8.62E+03	85.05
Luxembourg	1.12E+02	3.88E+01	21.80	3.97E+03	1.55E+03	27.09
Malaysia	1.19E+02	2.89E+01	10.35	8.35E+03	3.36E+03	71.40
Marocco	2.07E+02	7.59E+01	27.32	9.39E+03	3.54E+03	52.51
Netherlands	6.12E+03	2.27E+03	33.78	4.82E+04	1.77E+04	37.80
Niger	6.56E+01	4.64E+01	47.06	9.77E+02	3.03E+02	18.25
Norway	2.38E+02	9.25E+01	24.48	8.51E+03	2.98E+03	26.79
Portugal	1.65E+03	4.60E+02	24.47	3.69E+04	1.21E+04	36.00
San Marino	4.19E+01	1.45E+01	17.73	6.83E+02	4.04E+02	48.24
Sierra Leone	5.15E+01	2.38E+01	19.90	1.61E+03	6.13E+02	51.80
Slovenia	1.10E+02	4.11E+01	26.06	1.48E+03	6.20E+02	21.66
South Korea	2.74E+02	1.15E+02	31.52	1.11E+04	4.56E+03	41.59
Spain	2.77E+04	1.02E+04	30.55	2.37E+05	9.86E+04	60.11
Sweden	5.50E+03	1.90E+03	43.18	1.22E+05	4.16E+04	123.46
Switzerland	1.94E+03	7.61E+02	32.08	3.08E+04	1.18E+04	30.27
Tajikistan	4.86E+01	2.21E+01	9.25	5.36E+03	2.25E+03	20.71
Thailand	5.69E+01	2.46E+01	36.21	3.05E+03	1.38E+03	67.44
Tunesia	4.87E+01	1.39E+01	12.79	1.08E+03	4.13E+02	28.44
UK	4.27E+04	1.55E+04	41.10	3.10E+05	1.25E+05	80.74
UK: CI	4.59E+01	2.17E+01	23.44	5.58E+02	2.20E+02	23.41
UK: IM	2.37E+01	1.23E+01	20.75	3.34E+02	1.44E+02	16.91
UAE	2.91E+02	1.33E+02	44.36	5.81E+04	2.44E+04	109.48
Uruguay	2.42E+01	NA	NA	9.90E+02	6.18E+01	3.23
USA	1.25E+05	4.56E+04	52.73	2.40E+06	9.23E+05	94.86

Notes: t_{infl} is the solution of $y(t) = y_{infl}$ (we used only y_{infl} but reported tinfl for the sake of completeness); NA means no inflection point; otherwise as in Table 2.

expected once the peak had been reached? Thereby, countries that had comparably low peak counts (y_{infl}) had comparably low final counts at the end of the first wave (asymptotic limit y_{max}). While for both types of data (confirmed cases, fatalities) the correlation between peak size and final size was high (Spearman rho close to 1) and highly significant (Spearman rank test for independence: P-values close to 0), this correlation was associated to country size. To eliminate this dependency, we studied the ratios y_{max}/y_{infl} for the 98 time-series (Table 5).

Fig. 2 illustrates the use of the BP-model for this problem by the example of Burkina Faso: The blue dots represent the reported fatalities. To smoothen the data, we identified the best-fit trajectory of the best fitting BP-model (black curve). We then used this model curve to estimate the epidemic peak (red: inflection point) and the final size (red line: asymptotic limit). While the fit by the logistic growth curve (green) to the data was clearly poorer, its asymptotic limit did not differ significantly from that of the best-fit growth curve. However, the drawback of the logistic growth curve was its data-independent ratio $y_{max}/y_{infl} = 2$ (resulting in a clearly distinct estimate for the inflection point, see red dots in Fig. 2). Using the best-fit BP-model the ratio for final size over peak size was $y_{max}/y_{infl} = 2.6$.

Table 5
Further statistics (computed from the previous parameters).

Country	*fatalities*		*confirmed cases*		*CFR*
	$y_{max}/\max(y_i)$	y_{infl}/y_{max}	$y_{max}/\max(y_i)$	y_{infl}/y_{max}	
Andorra	1.01	4.03	0.89	2.48	6.9%
AU: NSW	1.00	1.67	0.98	2.13	1.6%
Austria	0.98	2.72	0.95	2.51	4.1%
Belgium	0.99	2.56	0.99	2.41	16.2%
Burkina Faso	1.01	2.63	1.04	3.72	5.7%
CAN: Alberta	1.02	2.38	0.95	1.98	2.2%
CAN: BC	1.09	2.79	0.99	2.47	6.7%
CAN: NS	1.00	2.48	0.99	1.90	5.9%
CAN: Ontario	1.05	2.68	1.09	2.46	7.3%
CAN: Quebec	1.14	2.77	1.08	2.43	10.3%
Chad	0.99	3.46	1.03	2.15	8.3%
China: Hubei	0.99	2.37	1.00	1.73	4.7%
Croatia	0.99	2.14	0.99	2.49	4.7%
Cuba	0.99	2.07	0.98	2.75	3.7%
Czechia	1.03	3.65	0.95	2.95	3.5%
Denmark	1.01	3.04	1.02	2.82	4.8%
Estonia	1.03	4.12	0.96	2.72	3.8%
Finland	1.00	2.27	1.03	2.42	4.4%
France	0.98	2.39	0.97	2.24	15.7%
Germany	1.00	2.64	0.97	2.40	4.9%
Greece	1.02	3.54	0.94	2.82	6.3%
Hungary	1.03	2.70	1.02	2.65	14.0%
Ireland	0.99	2.31	0.99	2.23	6.7%
Israel	1.00	3.08	0.86	2.43	1.8%
Italy	1.01	2.78	1.00	2.54	14.7%
Japan	1.03	2.09	0.96	1.96	5.7%
Luxembourg	1.02	2.89	0.97	2.56	2.8%
Malaysia	0.98	4.12	0.98	2.48	1.4%
Marocco	0.97	2.73	1.04	2.65	2.2%
Netherlands	1.01	2.69	0.98	2.72	12.7%
Niger	0.98	1.41	0.96	3.22	6.7%
Norway	0.98	2.58	0.98	2.85	2.8%
Portugal	1.08	3.58	0.98	3.06	4.5%
San Marino	1.00	2.90	0.98	1.69	6.1%
Sierra Leone	1.01	2.16	1.29	2.62	3.2%
Slovenia	1.00	2.66	0.98	2.39	7.4%
South Korea	0.98	2.38	0.91	2.43	2.5%
Spain	0.96	2.70	0.97	2.41	11.7%
Sweden	1.09	2.89	2.24	2.93	4.5%
Switzerland	0.99	2.55	0.99	2.60	6.3%
Tajikistan	0.95	2.20	1.03	2.39	0.9%
Thailand	0.98	2.31	0.97	2.20	1.9%
Tunesia	0.97	3.50	0.96	2.61	4.5%
UK	1.01	2.76	1.03	2.48	13.8%
UK: CI	0.96	2.12	0.98	2.53	8.2%
UK: IM	0.99	1.93	0.99	2.31	7.1%
UAE	0.99	2.19	1.34	2.39	0.5%
Uruguay	1.01	NA	1.17	16.02	2.4%
USA	1.06	2.73	1.11	2.60	5.2%

Notes: $\max(y_i)$ are the June 18 counts of Table 1; *CFR* is the case fatality rate and lower/upper are estimates for the minimal/maximal rates of other "good fitting" models (based on a simulation); otherwise as in Table 4.

For all 49 time-series of cumulated counts of confirmed infections, the best-fit BP-model had an inflection point and the ratios y_{max}/y_{infl} ranged from 1.7 to 16. The median of y_{max}/y_{infl} was 2.48 with lower and upper confidence limits 2.42 and 2.6 (one-sided sign-tests: P-value 2.2% for both limits and therefore confidence level 95.6%). For the cumulated counts of fatalities, the best-fit BP-model to the time-series of Uruguay was without inflection point. For the remaining 48 time-series, the ratios y_{max}/y_{infl} ranged from 1.42 to 4.12. The median of y_{max}/y_{infl} was 2.67 with lower and upper confidence limits 2.39 and 2.765 (one-sided sign-tests: P-values 2.97% and 1.47% for the lower and upper limit, respectively, and therefore confidence level 95.6%).

We note that the ratios y_{max}/y_{infl} were (stochastically) higher for the time-series of fatalities: Removing Uruguay temporarily from the dataset (no inflection point), 2/3 of the 48 remaining countries/provinces (i.e.: all, except nine) had a higher ratio y_{max}/y_{infl} for the fatalities than for the confirmed infections (one-sided sign-test: P-value 1.5%). Further, the ratios for the fatalities and confirmed infections were correlated (Spearman rho 0.332 with P-value 2.1% for the Spearman rank test of independence).

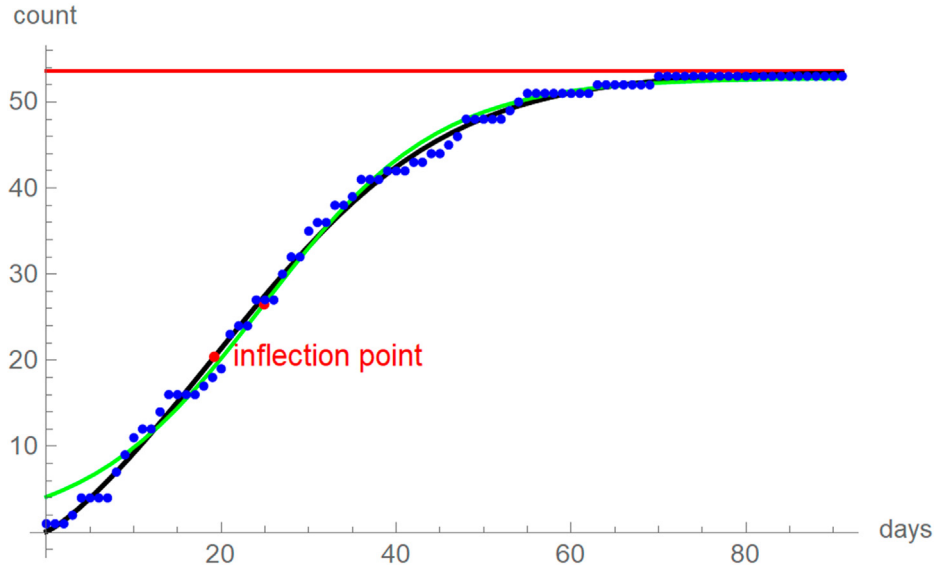

Fig. 2. Total count of deceased since the begin of the COVID-19 epidemics in Burkina Faso (blue dots), logistic growth curve (green), best-fit growth curve (black), asymptotic limit (red line), and inflection points (red dots) of the best-fit growth curve (labeled) and the logistic growth curve.

The distributions of the ratios y_{max}/y_{infl} differed between the samples of confirmed cases and fatalities (Anderson-Darling test for equal distributions: P-value 0.9%, using a smooth kernel distribution). However, two different Cauchy-distributions could be fitted to the samples (Anderson-Darling test: P-value 26.6% for the fatalities and 56.6% for the confirmed infections). Recall that the Cauchy distribution has the cumulative distribution function $CDF(x) = 0.5 + \arctan((x-m)/s)/\pi$. Using the maximum-likelihood parameters ($m = 2.6209$, $s = 0.272202$ for fatalities, $m = 2.4828$, $s = 0.154565$ for confirmed cases) we obtained the confidence intervals [1, 6.08], and [1, 4.447] for the ratios for fatalities and confirmed infections, respectively. (The upper limits are the 97.5% quantiles of the distributions. For the lower limits, always $y_{max}/y_{infl} \geq 1$. Note that compared to the cumulative histogram, *CDF* overestimated the probability of ratios below 2.)

Case fatality rates

The case fatality rate of a disease in a country is the number of dead over the number of diagnosed infections at a certain moment of time. When used for estimating the plausible lethality (*IFR*: infection fatality rate), there is a bias, as the count of recovered persons is not considered (Ghani et al., 2005) and as a correction for the time-lag between becoming infected and dying is needed (Russell et al., 2020). Further, for COVID-19 there is an additional uncertainty in view of the unknown number of asymptomatic infections that never have been identified. For this reason we considered a time-independent asymptotic version for the first wave of COVID-19 and we used it for country comparison (rather than for estimating *IFR*): *CFR* is the asymptotic limit of fatalities over the asymptotic limit of confirmed cases (Table 5).

CFR varied widely between the countries, from 0.5% for the United Arab Emirates to 16.2% for Belgium. The seven countries with the largest *CFR*-values were Spain (*CFR* = 11.7%), Netherlands (12.7%), United Kingdom (13.8%), Hungary (14%), Italy (14.7%), France (15.7%), and Belgium (16.2%).

The median *CFR* was 4.85% and the limits of the confidence interval for the median were 4.4% and 6.5%. (Using a one-sided sign-test the P-value was 2.22% for each limit, resulting in a confidence level of 95.6%.) Was the variability of *CFR* compatible with the hypothesis of random fluctuations? In other words, did a *CFR* above/below the median indicate a poor/good policy response? We observed that even the high *CFR*-values were within the range of statistical fluctuations of a lognormal distribution. Thereby first, for the full sample of 49 CFR-values the hypothesis that their logarithms were normally distributed was not refuted by the Anderson-Darling test (P-value 23.8%.) Second, assuming a lognormal distribution for *CFR*, we used the maximum likelihood-method to identify its location and shape parameters (−3.04606 and 0.731759, respectively; median 4.7546%). This resulted in the 95%-confidence interval for the *CFR*-values between 1.13% and 19.95%. The latter bound was higher than the highest observed *CFR*.

4. Conclusion

We have compared the experiences of different countries with the first wave of COVID-19, as this may help in shaping future responses.

As to our primary aim, we have shown that the general BP-model had excellent fits to the epidemiological data of the considered countries (Section 3.1). It clearly outperformed logistic growth. Based on 98 COVID-19 time-series the general BP-model achieved in the median $R^2 = 99.83\%$ with a narrow 95% confidence interval. As a caveat, we claim this good fit only for the problem of fitting the general BP-model to epidemic data that are cumulative and that include the after-peak stage. For our data, the latter condition was confirmed by the statistic "asymptotic limit over final count" (Section 3.2), whose median was close to one.

As to policy recommendations we found that countries that could keep the peak of the wave low succeeded also in keeping the final size low (Section 3.3). We confirmed this by modeling final size over peak size by the statistics "asymptotic limit over size at the inflection point". For the general BP-model this ratio was flexible and therefore (other than for logistic growth with a fixed ratio of 2) it could be estimated from the data. Thereby, our data would have supported the following forecasts for a country/province during the first wave of the COVID-19 epidemics: Using the medians, at the peak of the confirmed infections one could forecast that the final count of infections at the end of the wave would be about 2.5 times the present peak count. Further, at the peak of fatalities the forecast for the final count of fatalities would be 2.7 times the present peak count. Note that these forecasts extrapolated from the sample of 49 countries/provinces. As to limitations for such forecasts, we assumed that these countries would be representative for the global situation.

The case fatality rate, *CFR*, is another statistic of concern for epidemiologists (Section 3.4). Did a high *CFR* indicate a policy failure? The median *CFR* was about 5%, but for some countries it exceeded 10%. While it might be true that in countries with excessive *CFR* something might have gone wrong, our data were consistent with the hypothesis of a lognormal distribution for which high *CFR*-values were not unlikely. Thus, our data did not allow to single out countries with a particularly good or bad performance.

Declaration of competing interest

The authors declare no competing interests and there did not arise ethical issues, as we used ethically unproblematic data from open sources. Links to these data are provided in the paper.

References

Bertalanffy, L.v. (1957). Quantitative laws in metabolism and growth. *Quarterly Revues in Biology, 32*, 217–231.

Brody, S. (1945). *Bioenergetics and growth*. New York, NY, USA: Hafner Publ. Comp.

Brunner, N., & Tschohl, C. (2014). Do patterns of treaty ratifications reveal societal preferences? Analysis of twelve council of Europe conventions. In *Jusletter-IT, special issue: Proceedings of IRIS, 14-20 February 2014, Salzburg, Austria.* published online at the Link www.weblaw.ch.

Burnham, K. P., & Anderson, D. R. (2002). *Model selection and multi-model inference: A practical information-theoretic approach*. Berlin: Springer.

Burnham, K. P., & Anderson, D. R. (2004). Multi-model inference. Understanding AIC and BIC in model selection. *Sociological Methods & Research, 33*, 261–304.

Chowell, G. (2017). Fitting dynamic models to epidemic outbreaks with quantified uncertainty: A primer for parameter uncertainty, identifiability, and forecasts. *Infectious Disease Modelling, 2*, 379–398.

CSSE. (2020). *COVID-19 data repository by the center for systems science and engineering (CSSE)*. Baltimore, USA: Johns Hopkins University. Link https://github.com/CSSEGISandData/COVID-19. (Accessed 21 July 2020).

Díaz-Francés, E., & Rubio, F. J. (2013). On the existence of a normal approximation to the distribution of the ratio of two independent normal random variables. *Statistical Papers, 54*, 309–323.

1 Ferretti, L., Wymant, C., Kendall, M., Zhao, L., Nurtay, A., Abeler-Dörner, L., Parker, M., Bonsall, D., & Fraser, C. (2020). Quantifying SARS-CoV-2 transmission suggests epidemic control with digital contact tracing. *Science, 368*. https://doi.org/10.1126/science.abb6936. published online.

Ghani, A. C., Donnelly, C. A., Cox, D. R., Griffin, J. T., Fraser, C., Lam, T. H., Ho, L. M., Chan, W. S., Anderson, R. M., Hedley, A. J., & Leung, G. M. (2005). Methods for estimating the case fatality ratio for a novel, emerging infectious disease. *American Journal of Epidemiology, 162*, 479–486.

Gompertz, B. (1832). On the nature of the function expressive of the law of human mortality, and on a new mode of determining the value of life contingencies. *Philosophical Transactions of the Royal Society of London, 123*, 513–585.

Hathaway, O. A. (2002). Do human rights treaties make a difference? *The Yale Law Journal, 111*, 1935–2042.

Hollander, M., & Wolfe D, A. (1999). *Nonparametric statistical methods*. Chichester, UK: Wiley.

Kamrujjaman, M., Shahriar, M., & Shafiqul, I. (2020). Coronavirus outbreak and the mathematical growth map of COVID-19. *Annual Research & Review in Biology, 35*, 72–78.

Kühleitner, M., Brunner, N., Nowak, W. G., Renner-Martin, K., & Scheicher, K. (2019). Best-fitting growth curves of the von Bertalanffy-Pütter type. *Poultry Science, 98*, 3587–3592.

Li, R., Pei, S., Chen, B., Song, Y., Zhang, T., Yang, W., & Shaman, J. (2020). Substantial undocumented infection facilitates the rapid dissemination of novel coronavirus (SARS-CoV-2). *Science, 368*, 489–493.

Magesan, A. (2013). Human rights treaty ratification of aid receiving countries. *World Development, 45*, 175–188.

Marusic, M., & Bajzer, Z. (1993). Generalized two-parameter equations of growth. *Journal of Mathematical Analysis and Applications, 179*, 446–462.

Motulsky, H., & Christopoulos, A. (2003). *Fitting models to biological data using linear and nonlinear regression: A practical guide to curve fitting*. Oxford, U.K: Oxford University Press.

Ohnishi, S., Yamakawa, T., & Akamine, T. (2014). On the analytical solution for the Pütter-Bertalanffy growth equation. *Journal of Theoretical Biology, 343*, 174–177.

Pütter, A. (1920). Studien über physiologische Ähnlichkeit. *VI. Wachstumsähnlichkeiten. Pflügers Archiv für die Gesamte Physiologie des Menschen und der Tiere, 180*, 298–340.

Remuzzi, A., & Remuzzi, G. (2020). COVID-19 and Italy: What next? *The Lancet, 395*, 1225–1228.

Renner-Martin, K., Brunner, N., Kühleitner, M., Nowak, W. G., & Scheicher, K. (2018). Optimal and near-optimal exponent-pairs for the Bertalanffy-Pütter growth model. *PeerJ, 6*. https://doi.org/10.7717/peerj.5973. published online.

Richards, F. J. (1959). A flexible growth function for empirical use. *Journal of Experimental Botany, 10*, 290–300.

Roosa, K., Lee, Y., Luo, R., Kirpich, A., Rothenberg, R., Hyman, J. M., Yan, P., & Chowell, G. (2020). Short-term forecasts of the COVID-19 epidemic in Guangdong and Zhejiang, China: February 13–23, 2020. *Journal of Clinical Medicine, 9*. https://doi.org/10.3390/jcm9020596. published online.

Russell, T. W., Hellewell, J., Jarvis, C. I., van Zandvoort, K., Abbott, S., Ratnayake, R., Cmmid Covid-Working Group, Flasche, S., Eggo, R. M., Edmunds, W. J., & Kucharski, A. J. (2020). Estimating the infection and case fatality ratio for coronavirus disease (COVID-19) using age-adjusted data from the outbreak on

the Diamond Princess cruise ship, February 2020. *Euro Surveillance: European Communicable Disease Bulletin, 25*. https://doi.org/10.2807/1560-7917.ES.2020.25.12.2000256. published online.

Shen, C. Y. (2020). Logistic growth modelling of COVID-19 proliferation in China and its international implications. *International Journal of Infectious Diseases, 96*, 582–589.

Sornette, D., Mearns, E., Schatz, M., Wu, K., & Darcet, D. (2020). *Interpreting, analyzing and modelling COVID-19 mortality data*. https://doi.org/10.2139/ssrn.3586411. Preprint published online.

Spiess, A. N., & Neumeyer, N. (2010). An evaluation of R^2 as an inadequate measure for nonlinear models in pharmacological and biochemical research: A Monte Carlo approach. *BMC Pharmacology, 10*. https://doi.org/10.1186/1471-2210-10-6. published online.

Tjørve, K. M. C., & Tjørve, E. (2017). A proposed family of unified models for sigmoidal growth. *Ecological Modelling, 359*, 117–127.

Vattay, G. (2020). *Predicting the ultimate outcome of the COVID-19 outbreak in Italy*. preprint published online: arXiv:2003.07912v2 [q-bio.PE].

Verhulst, P. F. (1838). Notice sur la loi que la population suit dans son accroissement. *Correspondence in Mathematics and Physics, 10*, 113–121.

Vidal, R. V. V. (1993). *Applied simulated annealing. Lecture notes in economics and mathematical systems*. Berlin: Springer-Verlag, 1993.

WHO. (2020). Coronavirus disease 2019 (COVID-19). Situation report No 73. last visit www.who.int. (Accessed 25 July 2020).

Wu, K., Darcet, D., Wang, Q., & Sornette, D. (2020). Generalized logistic growth modeling of the COVID-19 outbreak in 29 provinces in China and in the rest of the world. *Nonlinear Dynamics*. https://doi.org/10.1007/s11071-020-05862-6. see also the preprint DOI 10.1101/2020.03.11.20034363.

Ziegler, M. K., Brunner, N., & Kühleitner, M. (2020). The markets of green cars of three countries: Analysis using Lotka-Volterra and Bertalanffy-Pütter models. *Journal of Open Innovation: Technology, Market and Complexity*. https://doi.org/10.3390/joitmc6030067. published online.